Pion-⁴⁰Ca and Pion-⁴⁸Ca Elastic Scattering and the Neutron Radius of ⁴⁸Ca

J.-P. Egger, R. Corfu, P. Gretillat, C. Lunke, J. Piffaretti, and E. Schwarz

Institut de Physique, Université de Neuchâtel, CH-2000 Neuchâtel, Switzerland

and

C. Perrin

Institut des Sciences Nucléaires, Université de Grenoble, Centre de Tri, F-38044 Grenoble-Cedex, France

and

J. Jansen

Schweizerisches Institut für Nuklearforschung, CH-5234 Villigen, Switzerland

and

B. M. Preedom

University of South Carolina, Columbia, South Carolina, and Schweizerisches Institut für Nuklearforschung,
CH-5234 Villigen, Switzerland

π^+ and π^- data were obtained for scattering off ⁴⁰Ca and ⁴⁸Ca at 130 MeV. The ⁴⁸Ca angular distributions showed important π^+-π^- cross-section differences as well as significant position shifts of the cross-section minima, thereby indicating the sensitivity of pions for investigating neutron radii of nuclei.

A comparison of π^+ and π^- scattering in the region of the πN (3, 3) resonance is an ideal tool for investigating peripheral distributions of neutrons of nuclei, since π^+ are believed to interact preferentially with the protons, and π^- with neutrons of the nucleus. In this Letter we present the first comparison of elastic π^+ and π^- data on ⁴⁸Ca and ⁴⁰Ca. At an incident pion energy of 130 MeV, large $\pi^+\pi^-$ cross-section differences were seen for ⁴⁸Ca at the minima of the angular distributions. However, π^+-π^- differences in ⁴⁰Ca were less pronounced and can be reproduced by Coulomb distortion effects similar to those introduced by Germond and Wilkin[1] to explain our ¹²C data.[2] The remaining discrepancies between the π^+ and π^- scattering off ⁴⁸Ca, together with the charge radius obtained from electron scattering data,[3] should permit extraction of a neutron radius for ⁴⁸Ca. It is interesting to note that the electron scattering experiment of Ref. 3 found a very small ⁴⁸Ca-⁴⁰Ca charge-radius difference (−0.5%) in contradiction with the $A^{1/3}$ rule (standard isotopic shift) which predicts 0.22 fm (+6.3%) for the ⁴⁸Ca-⁴⁰Ca charge-radius difference. Assuming the matter radii also follow the $A^{1/3}$ rule, the neutron radius of ⁴⁸Ca would exceed the measured charge radius by 0.4 fm, which is in agreement with some theoretical work based on shell-model calculations.[4] However, Hartree-Fock calculations predict lower values around 0.2 fm.[5]

The experiment was carried out at the Swiss Institute of Nuclear Research (SIN) with the $\pi M1$ beam and pion spectrometer. Typical running conditions with a primary proton beam of ~40 μA were $2\times10^6 \pi^+$/s and $2\times10^5 \pi^-$/s incident on a 250-mg/cm² 92%-enriched ⁴⁸Ca target and on a 300-mg/cm² natural-calcium target. Momentum range of the incident pion beam was $\Delta p/p = \pm1.4\%$. A standard layout was used with six multiwire proportional chamber; two of them were in the beam line with a fast digital readout to allow the determination of the incident momentum and the angle incident on target. Change over from π^+ to π^- was achieved by reversing polarity of all beam and spectrometer elements. Protons in the beam were removed with an electrostatic separator. Muons and electrons were accounted for by a beam-sampling method allowing continuous monitoring of the beam composition. Muons from π decay in the spectrometer were largely rejected by imposing ion optical conditions on each particle trajectory. Overall relative momentum resolution was 2×10^{-3} full width at half-maximum (FWHM), which allowed for a clear separation of the elastic states from the inelastic states. A typical spectrum is shown in Fig. 1. The results of our analysis yield elastic angular distributions between 24° and 102° for ⁴⁰Ca and between 24° and 126° for ⁴⁸Ca. Since the pion spectrometer has an angular acceptance of 8°
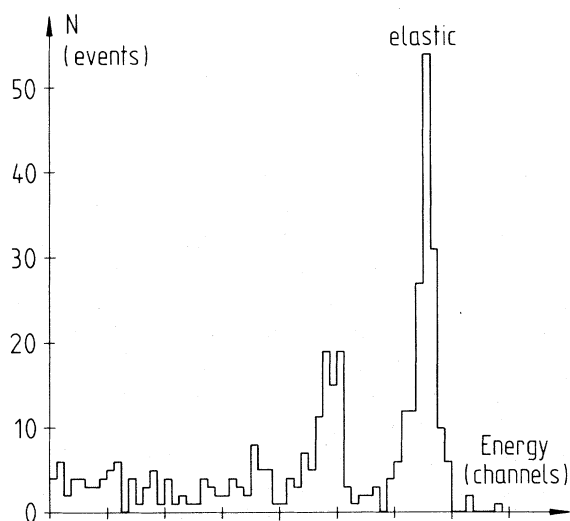
FIG. 1. Typical pion-scattering spectrum for 130-MeV π^+ at a lab angle of 81°.

FWHM, the data were divided into angular bins of 2°. Because the minima in the cross section are relatively deep, a finite-angle correction was
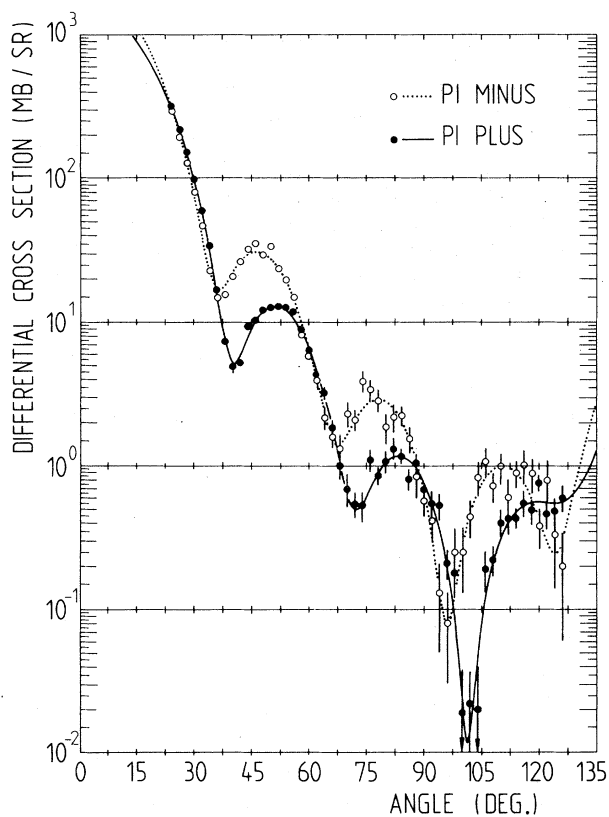
FIG. 3. Comparison of π^+- and π^--^{48}Ca elastic scattering differential cross sections at 130 MeV vs the pion scattering angle in the lab system. The curves result from a fit by a formula given in the text.
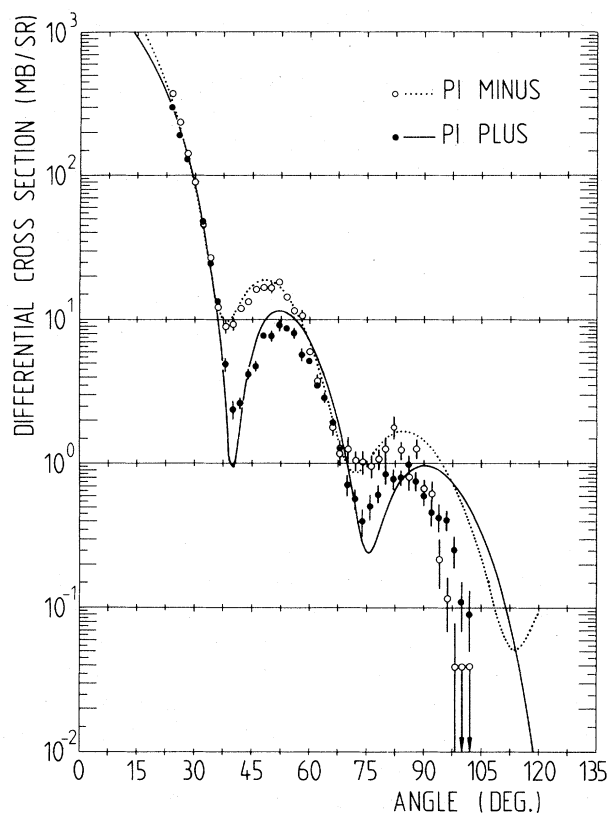
FIG. 2. Comparison of π^+- and π^--^{40}Ca elastic scattering differential cross sections at 130 MeV vs the pion scattering angle in the lab system. The curves are the results of a calculation with an α-particle model by Germond and Wilkin (Ref. 8).

performed which is similar to the finite-angle correction introduced by Binon et al.[6] Measurements were taken at 6° intervals, thus giving overlapping bins. The relative differences of two bins at the same scattering angle for two spectrometer positions were consistently compatible with statistics. Relative normalization between π^+ and π^- data was obtained, taking beam composition into account. For normalization purposes, measurements were also gathered with a polyethylene [$(CH_2)_n$] target. Scaling our data against the known hydrogen[7] and carbon[2,6] cross sections yielded the cross-section values presented.

The angular distributions are given in Figs. 2 and 3. No subtraction of background was required; error bars are statistical. The absolute normalization error was estimated at ±5%. In the case of ^{48}Ca, the π^+-π^- cross sections near the minima of the angular distributions differ up to a factor of 4. In addition the position of the

first minimum is shifted by $4°$ towards smaller angles for π^-. The shift is $5°$ for the position of the second minimum. These shifts as well as the important cross-section differences are believed to be due partially to the larger neutron distribution in ^{48}Ca. The ^{40}Ca angular distributions show smaller differences and a smaller shift of the minima ($2°$ for the first minimum and ~$2°$ for the second minimum).

For both isotopes the elastic data were fitted independently for π^+ and π^- with a scattering amplitude of the form

$$f(z) = f(z=1)\left(\prod_{i=1}^{4} \frac{z - z_i}{1 - z_i}\right)e^{-\alpha(1-z)},$$

where $z = \cos\theta_{lab}$. Thus the amplitude depends on the nearby complex zeros z_i, the forward-scattering amplitude $f(z=1)$ and a slope parameter α. The parameters of the fit are given in Table I. This fit, which facilitates the determination of the position of the minima, is a convenient representation of the data in view of a detailed analysis. This type of analysis was already used to reproduce the data of Refs. 2 and 6. In addition, a calculation was performed for ^{40}Ca based on an α-particle model as described by Germond and Wilkin.[8] Furthermore, a crude estimate of the ^{48}Ca-^{40}Ca radius difference was made using the simple black-disk model, where the scattering amplitude is $f(\theta) = ikR^2[J_1(qR)/qR]$ and $q = 2k \sin(\theta/2)$. With $J_1(x) = 0$ for $x = 3.83$ (first minimum) and $k = 1.17$ fm^{-1}, the values obtained for the π^--

π^+ radius difference ΔR are

$$\Delta R_{\mp} = R(\pi^-) - R(\pi^+) = 0.21 \text{ fm for } ^{40}\text{Ca},$$

$$\Delta R_{\mp} = R(\pi^-) - R(\pi^+) = 0.51 \text{ fm for } ^{48}\text{Ca}.$$

By subtraction of the two differences, the Coulomb effects are taken into account in an empirical way. Thus a ^{48}Ca-^{40}Ca radius difference of 0.3 fm is obtained. Bethe and Johnson[9] have improved this model, taking into account the diffuseness of the nuclear surface; for π^-, R becomes the radius for which $(\frac{1}{2}\rho_p + \frac{3}{2}\rho_n)/\rho_0 = 0.2$, where ρ_0 is the central density equal to 0.16 fm^{-3}. They find a radius difference of ~0.3 fm, consistent with Negele's density distributions.[5] The total-cross-section experiments for ^{40}Ca and ^{48}Ca [10] were analyzed for the rms-radius difference and this quantity came out smaller than in Ref. 5.

We wish to thank the crew of the SIN machine for their efficient operation of the accelerator. This work was supported in part by the Swiss National Science Foundation and the U. S. National Science Foundation.

[1]J.-F. Germond and C. Wilkin, Phys. Lett. 68B, 229 (1977), and private communication.

[2]J. Piffaretti, R. Corfu, J.-P. Egger, P. Gretillat, C. Lunke, E. Schwarz, and C. Perrin, Phys. Lett. 67B, 289 (1977), and to be published.

[3]R. F. Frosch, R. Hofstadter, J. S. McCarthy, G. K. Nöldeke, K. J. vanOostrum, M. R. Yearian, B. C. Clark, R. Herman, and D. G. Ravenhall, Phys. Rev. 174, 1380 (1968).

TABLE I. Parameters deduced by fitting the formula given in the text to the calcium data at 130 MeV separately for π^+ and π^- in the lab system, together with the χ^2 per degree of freedom (χ^2/N).

	Nucleus	$\frac{d\sigma}{d\Omega}$ (θ=0) lab (mb/sr)	α	Re z_1	Im z_1	Re z_2	Im z_2	Re z_3	Im z_3	Re z_4	Im z_4	χ^2/N
π^+	^{40}Ca	1603 ± 40	2.62 ± 0.06	.762 ± .001	-.0296 ± .0014	.296 ± .005	-.0943 ± .0057	-.244 ± .035	-.0618 ± .0276	——	——	1.31
π^-	^{40}Ca	2460 ± 80	2.96 ± 0.07	.793 ± .001	-.0404 ± .0013	.347 ± .004	-.0968 ± .0061	-.179 ± .009	-.0209 ± .0227	——	——	1.20
π^+	^{48}Ca	1691 ± 28	1.53 ± 0.05	.769 ± .001	-.0410 ± .0010	.313 ± .004	-.0704 ± .0056	-.198 ± .005	-.0229 ± .0147	-.626 ± .036	.131 ± .012	1.43
π^-	^{48}Ca	2352 ± 66	1.83 ± 0.05	.816 ± .001	-.0452 ± .0012	.396 ± .004	-.0737 ± .0043	-.103 ± .006	-.0400 ± .0106	-.566 ± .011	-.0579± .0120	2.19

[4]L. R. Elton and A. Swift, Nucl. Phys. A94, 52 (1967); C. J. Batty and G. W. Greenless, Nucl. Phys. A133, 673 (1969).

[5]J. W. Negele, Phys. Rev. C 1, 1260 (1970); D. Vautherin and D. M. Brink, Phys. Lett. 32B, 149 (1970); H. C. Lee and R. Y. Cusson, Nucl. Phys. A170, 439 (1971); R. J. Lombard, Phys. Lett. 32B, 652 (1970); R. C. Barrett, Rep. Prog. Phys. 37, 1 (1974), and J. Phys. (Paris), Colloq. C4, 23 (1973).

[6]F. Binon, P. Duteil, J.-P. Garron, J. Gorres, L. Hugon, J.-P. Peigneux, C. Schmit, M. Spighel, and J.-P. Stroot, Nucl. Phys. B17, 168 (1970).

[7]J. Ashkin, J.-P. Blaser, F. Feiner, and M. O. Stern,

Phys. Rev. 101, 1149 (1956); P. J. Bussey, J. R. Carter, D. R. Dance, D. V. Bugg, A. A. Carter, and A. M. Smith, Nucl. Phys. B58, 363 (1973).

[8]J.-F. Germond and C. Wilkin, Nucl. Phys. A249, 457 (1975).

[9]Hans A. Bethe and Mikkel B. Johnson, LASL Report No. LA-UR-76-1844, 1976 (unpublished), and private communication.

[10]M. J. Jakobson, G. R. Burleson, J. R. Calarco, M. D. Cooper, D. C. Hagerman, I. Halpern, R. H. Jeppeson, K. F. Johnson, L. D. Knutson, R. E. Marrs, H. O. Meyer, and R. P. Redwine, Phys. Rev. Lett. 38, 1201 (1977).

Analysis of the Lamp-Dip Structure with Linear and Helicoidal Polarizations

A. Le Floch

Laboratoire d'Electronique Quantique, Université de Rennes, 35031 Rennes Cedex, France

and

R. Le Naour

Laboratoire d'Electronique Quantique, Université de Nantes, 44037 Nantes Cedex, France

and

G. Stephan

Institut de Physique, Université d'Oran, Oran, Algérie

A simple differential analysis of the Lamb-dip structure using a stationary helicoidal wave is described. This technique enables us to separate the anisotropic contribution from the isotropic one and shows that the observed Lamb dip on the 3.39-μm line of Ne^{20} is partially anisotropic.

The Lamb dip predicted by Lamb's self-consistency theory[1] has been studied by many authors, both experimentally[2] and theoretically.[3] The usual observation is performed on the output power of a linearly polarized monomode laser. This resonance at the center of a Doppler profile is described in the scalar theory as a Lorentzian of width $2\gamma_{ab}$. The "hole-burning" concept introduced by Bennett[4] gives a simple phenomenological interpretation of the resonance by merging at line center of two atomic packets which interact with the two progressive waves of the stationary mode. In a recent probe experiment[5] on the active column of an He-Ne laser, we have directly shown and measured the induced anisotropies occurring in the "atoms + field" system. That is to say, we have isolated the anisotropic contribution of the saturation depending on the level degeneracies which were previously considered in Zeeman laser theory.[6] We describe a new experiment using a stationary helicoidal wave on the 3.39-μm line of Ne^{20} which allows the study of the Lamb-

dip structure by observation of its isotropic and anisotropic parts. This simple differential analysis shows that, on this particular line, the Lamb dip is partially anisotropic and necessitates an interpretation in the spatial vectorial model,[7] even in zero magnetic field. According to Bennett's physical interpretation of the Lamb dip, it is then necessary to introduce the concept of "aligned holes."

The scheme of the apparatus is shown in Fig. 1(a). A monomode laser with a stationary field having either a linear or a helicoidal structure is realized. When both slow axes of the $\lambda/4$ plates are in the incidence plane of the Brewster window, the polarization of the field is linear [Fig. 1(b)] all along the laser. On the contrary, if the $\lambda/4$ plate No. 1 is rotated through $\pm 45°$, the stationary field in the active medium between the two plates is represented by either a right-handed or a left-handed helix [Fig. 1(c)]; this field configuration has been proposed by Evtuhov and Siegman[8] and by Kastler,[9] and has been experimental-